Load-Flow in Multiphase Distribution Networks: Existence, Uniqueness, and Linear Models

Andrey Bernstein, Cong Wang, Emiliano Dall'Anese, Jean-Yves Le Boudec, and Changhong Zhao

arXiv:1702.03310v1 [math.OC] 10 Feb 2017

***Abstract*—This paper considers generic unbalanced and multiphase distribution systems and develops a load-flow algorithm based on a fixed-point interpretation of the AC power-flow equations. Explicit conditions for existence and uniqueness of load-flow solutions are presented. These conditions also guarantee convergence of the load-flow algorithm to the unique power-flow solution. The proposed methodology broadens the well-established Z-bus iterative method, and it is applicable to generic systems featuring (i) wye connections; (ii) ungrounded delta connections; (iii) a combination of wye-connected and delta-connected sources/loads; and, (iv) a combination of line-to-line and line-to-grounded-neutral devices at the secondary of distribution transformers. Linear load-flow models are then derived, and their approximation accuracy is analyzed. Theoretical results are corroborated through experiments on IEEE test feeders.**

I. Introduction

Load-flow analysis is a fundamental task in power systems theory and applications. In this paper, we consider a load-flow problem for a multiphase distribution network. The network has a generic topology (it can be either radial or meshed), it has a single slack bus with voltages that are fixed and known, and it features multiphase PQ buses. At each multiphase bus, the model of the distribution system can have: (i) grounded wye-connected loads/sources; (ii) ungrounded delta connections; (iii) a *combination* of wye-connected and delta-connected loads/sources; or, (iv) a *combination* of line-to-line and line-to-grounded-neutral devices at the secondary of distribution transformers [1]. Models (i)–(iii) pertain to settings when the network model is limited to (aggregate) nodal power injections at the primary side of distribution transformers. Particularly, the combined model (iii) can be utilized when different distribution transformers with either delta and/or wye primary connections are bundled together at one bus for network reduction purposes (e.g., when two transformers are connected through a short low-impedance distribution line); see Figure 1(a) for an illustration. Load model (iv) is common in, e.g., North America for commercial buildings and residential customers, and it can be utilized when the network model includes the secondary of the distribution transformers; see an illustrative example in Figure 1(b) and low-voltage test feeders available in the literature (e.g., the IEEE 342-Node Low-Voltage Test System). Settings with only line-line or line-ground connections at the secondary are naturally subsumed by model (iv).

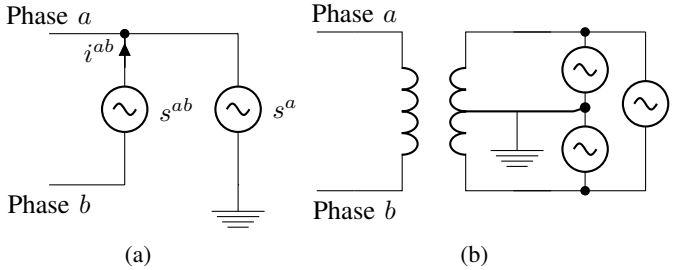

Fig. 1: Examples of a multiphase point of connection (for illustration simplicity, only two phases are shown): (a) Combination of wye-connected and delta-connected loads/sources at the primary of the feeder (due to e.g., network reduction procedures). (b) Combination of line-to-line loads/sources and line-to-grounded-neutral devices at the secondary of distribution transformer.

Due to the nonlinearity of the AC power-flow equations, the existence and uniqueness of the solution to the load-flow problem is not guaranteed in general [2]–[4]. Recently, solvability of lossless power-flow equations was investigated in [5]. Focusing on the AC power-flow equations, several efforts investigated explicit conditions for existence and uniqueness of the (high-voltage) solution in balanced distribution networks [6]–[8] as well as in the more realistic case of unbalanced three-phased networks [9], [10].

This paper examines the load-flow problem for generic multiphase distribution systems with load models (i)–(iv), and outlines a load-flow iterative solution method that augments classical Z-bus methodologies [11], [12]. The iterative algorithm is obtained by leveraging the fixed-point interpretation of the nonlinear AC power-flow equations in [8]. We give explicit conditions that guarantee the existence and uniqueness of the load-flow solution. Under the satisfaction of these conditions, it is shown that the proposed algorithm achieves this unique solution. Compared to existing methods and analysis (including the classical Z-bus method), the contribution is twofold:

- When only the load models (i)–(ii) are utilized (and for settings with only line-line or line-ground connections at the secondary), the analytical conditions for convergence presented in this paper improve upon existing methods [9], [10] by providing an enlarged set of power profiles that guarantee convergence.
- The methods and analysis outlined in [9], [10] are not applicable when the load models (iii) and (iv) are utilized. On the other hand, this paper provides a unified

Andrey Bernstein, Emiliano Dall'Anese, and Changhong Zhao are with the National Renewable Energy Laboratory (NREL), Golden, CO, USA. Cong Wang and Jean-Yves Le Boudec are with Ecole Polytechnique Federale de Lausanne (EPFL), Lausanne, Switzerland.

This work was supported by the U.S. Department of Energy under Contract No. DE-AC36-08GO28308 with the National Renewable Energy Laboratory. The U.S. Government retains and the publisher, by accepting the article for publication, acknowledges that the U.S. Government retains a nonexclusive, paid-up, irrevocable, worldwide license to publish or reproduce the published form of this work, or allow others to do so, for U.S. Government purposes.

load-flow solution method for general loads models at both the primary and secondary sides of the distribution transformer. To the best of our knowledge, the only existing freely available load-flow solver for networks with all models (i)–(iv) is part of the OpenDSS platform [13]. However, the details of the algorithm utilized in OpenDSS as well as its convergence analysis are not available in the literature.

The paper then presents approximate load-flow models to relate voltages and complex power injections through an approximate linear relationship. The development of approximate linear models is motivated by the need of computationally-affordable optimization and control applications – from advanced distribution management systems settings to online and distributed optimization routines. For example, the nonlinearity of the (exact) AC power-flow equations poses significant difficulties in solving AC optimal power flow (OPF) problems [14], [15]. Typical approaches involve convex relaxation methods (e.g., semidefinite program [14]) or a linearization of the power-flow equation [16]–[18]. Approximate linear models have been recently utilized to develop real-time OPF solvers for distribution systems [19], [20]. The methodology proposed in the present paper is applicable to generic multiphase networks, and it can be utilized to broaden the applicability of [15], [19], [20].

Notation: Upper-case (lower-case) boldface letters are used for matrices (column vectors); $(\cdot)^{\mathsf{T}}$ for transposition; $|\cdot|$ for the absolute value of a number or the element-wise absolute value of a vector or a matrix; and the letter $\jmath$ for $\jmath := \sqrt{-1}$. For a complex number $c \in \mathbb{C}$, $\Re\{c\}$ and $\Im\{c\}$ denote its real and imaginary part, respectively; and $\overline{c}$ denotes the conjugate of c. For a given $N \times 1$ vector $\mathbf{x} \in \mathbb{C}^N$, $\|\mathbf{x}\|_\infty := \max(|x_1|...|x_n|)$, $\|\mathbf{x}\|_1 := \sum_{i=1}^N |x_i|$, and $\mathsf{diag}(\mathbf{x})$ returns a $N \times N$ matrix with the elements of $\mathbf{x}$ in its diagonal. For an $M \times N$ matrix $\mathbf{A} \in \mathbb{C}^{M\times N}$, the ℓ_∞-induced norm is defined as $||\mathbf{A}||_\infty = \max_{i=1,...,M} \sum_{j=1}^N |\mathbf{A}_{ij}|$. Finally, for a vector-valued map $\mathbf{x} : \mathbf{y} \in \mathbb{R}^{N\times 1} \to \mathbf{x}(\mathbf{y}) \in \mathbb{C}^{M\times 1}$, we let $\partial\mathbf{x}/\partial\mathbf{y}$ denote the $M \times N$ complex matrix with elements $(\partial\mathbf{x}/\partial\mathbf{y})_{ik} = \partial\mathbf{x}_i/\partial\mathbf{y}_k = \partial\Re\{\mathbf{x}_i\}/\partial\mathbf{y}_k + \jmath\partial\Im\{\mathbf{x}_i\}/\partial\mathbf{y}_k$, $i = 1,\dots,M$, $k = 1,\dots,N$.

II. Problem Formulation

For notational simplicity, the framework is outlined for three-phase systems; we describe in Remark 1 below how to apply the analysis to the general multiphase case (as we do in the numerical examples in Section V-B). Consider a generic three-phase distribution network with one slack bus and N three-phase PQ buses. With reference to the illustrative example in Figure 1, let $\mathbf{s}_j^Y := (s_j^a, s_j^b, s_j^c)^{\mathsf{T}}$ denote the vector of grounded wye sources at node j, where $s_j^\phi \in \mathbb{C}$ denotes the net complex power injected on phase ϕ. Similarly, let $\mathbf{s}_j^\Delta := (s_j^{ab}, s_j^{bc}, s_j^{ca})^{\mathsf{T}}$ denote the power injections of delta-connected sources. With a slight abuse of notation, $\mathbf{s}_j^Y$ and $\mathbf{s}_j^\Delta$ will represent line-line connections and line-ground connections, respectively, when bus j corresponds to the secondary side of the distribution transformer (this notational choice allows us not to introduce additional symbols).

At bus j, the following set of equations relates voltages, currents, and powers:

$$\begin{aligned} s_j^{ab} &= (v_j^a - v_j^b)\overline{i_j^{ab}}, & v_j^a(\overline{i_j^{ab}} - \overline{i_j^{ca}}) + s_j^a &= v_j^a\overline{i_j^a},\\ s_j^{bc} &= (v_j^b - v_j^c)\overline{i_j^{bc}}, & v_j^b(\overline{i_j^{bc}} - \overline{i_j^{ab}}) + s_j^b &= v_j^b\overline{i_j^b},\\ s_j^{ca} &= (v_j^c - v_j^a)\overline{i_j^{ca}}, & v_j^c(\overline{i_j^{ca}} - \overline{i_j^{bc}}) + s_j^c &= v_j^c\overline{i_j^c}, \end{aligned}$$

where $\mathbf{v}_j = (v_j^a, v_j^b, v_j^c)^{\mathsf{T}}$, $\mathbf{i}_j = (i_j^a, i_j^b, i_j^c)^{\mathsf{T}}$, and $\mathbf{i}_j^\Delta = (i_j^{ab}, i_j^{bc}, i_j^{ca})^{\mathsf{T}}$ collect the phase-to-ground voltages $\{v_j^\phi\}_{\phi\in\{a,b,c\}}$, phase net current injections $\{i_j^\phi\}_{\phi\in\{a,b,c\}}$, and phase-to-phase currents $\{i_j^{\phi\phi'}\}_{\phi,\phi'\in\{a,b,c\}}$ (for delta connections and line-line connections) of node j, respectively.

We next express the set of power-flow equations in vector-matrix form. To this end, let $\mathbf{v}_0 := (v_0^a, v_0^b, v_0^c)^{\mathsf{T}}$ denote the complex vector collecting the three-phase voltages at the slack bus (i.e., the substation). Also, let $\mathbf{v} := (\mathbf{v}_1^{\mathsf{T}}, \dots, \mathbf{v}_N^{\mathsf{T}})^{\mathsf{T}}$, $\mathbf{i} := (\mathbf{i}_1^{\mathsf{T}}, \dots, \mathbf{i}_N^{\mathsf{T}})^{\mathsf{T}}$, $\mathbf{i}^\Delta := ((\mathbf{i}_1^\Delta)^{\mathsf{T}}, \dots, (\mathbf{i}_N^\Delta)^{\mathsf{T}})^{\mathsf{T}}$, $\mathbf{s}^Y := ((\mathbf{s}_1^Y)^{\mathsf{T}}, \dots, (\mathbf{s}_N^Y)^{\mathsf{T}})^{\mathsf{T}}$, and $\mathbf{s}^\Delta := ((\mathbf{s}_1^\Delta)^{\mathsf{T}}, \dots, (\mathbf{s}_N^\Delta)^{\mathsf{T}})^{\mathsf{T}}$ be the vectors in $\mathbb{C}^{3N}$ collecting the respective electrical quantities of the PQ buses. The load-flow problem is then defined as solving for $\mathbf{v}$ (and $\mathbf{i}^\Delta$) in the following set of equations, where $\mathbf{s}^Y$, $\mathbf{s}^\Delta$, and $\mathbf{v}_0$ are given:

$$\mathsf{diag}\left(\mathbf{H}^{\mathsf{T}}\overline{\mathbf{i}^\Delta}\right)\mathbf{v} + \mathbf{s}^Y = \mathsf{diag}(\mathbf{v})\overline{\mathbf{i}}, \tag{1a}$$

$$\mathbf{s}^\Delta = \mathsf{diag}\left(\mathbf{H}\mathbf{v}\right)\overline{\mathbf{i}^\Delta}, \tag{1b}$$

$$\mathbf{i} = \mathbf{Y}_{L0}\mathbf{v}_0 + \mathbf{Y}_{LL}\mathbf{v}. \tag{1c}$$

In (1), $\mathbf{Y}_{00} \in \mathbb{C}^{3\times 3}, \mathbf{Y}_{L0} \in \mathbb{C}^{3N\times 3}, \mathbf{Y}_{0L} \in \mathbb{C}^{3\times 3N}$, and $\mathbf{Y}_{LL} \in \mathbb{C}^{3N\times 3N}$ are the submatrices of the three-phase admittance matrix

$$\mathbf{Y} := \begin{bmatrix} \mathbf{Y}_{00} & \mathbf{Y}_{0L} \\ \mathbf{Y}_{L0} & \mathbf{Y}_{LL} \end{bmatrix} \in \mathbb{C}^{3(N+1)\times 3(N+1)}, \tag{2}$$

which can be formed from the topology of the network and the π-model of the distribution lines, as shown in, e.g., [1]; and $\mathbf{H}$ is a $3N \times 3N$ block-diagonal matrix defined by

$$\mathbf{H} := \begin{bmatrix} \mathbf{\Gamma} & & \\ & \ddots & \\ & & \mathbf{\Gamma} \end{bmatrix}, \quad \mathbf{\Gamma} := \begin{bmatrix} 1 & -1 & 0 \\ 0 & 1 & -1 \\ -1 & 0 & 1 \end{bmatrix}. \tag{3}$$

By simple algebraic manipulations, it can be seen that the solution $\mathbf{v}$ to the set (1) can be found from the following fixed-point equation:

$$\begin{aligned} \mathbf{v} &= \mathbf{G}_{\mathbf{s}^Y\mathbf{s}^\Delta}(\mathbf{v}) \\ &:= \mathbf{w} + \mathbf{Y}_{LL}^{-1}\left(\mathsf{diag}(\overline{\mathbf{v}})^{-1}\overline{\mathbf{s}}^Y + \mathbf{H}^{\mathsf{T}}\mathsf{diag}\left(\mathbf{H}\overline{\mathbf{v}}\right)^{-1}\overline{\mathbf{s}}^\Delta\right), \end{aligned} \tag{4}$$

where[1] $\mathbf{w} := -\mathbf{Y}_{LL}^{-1}\mathbf{Y}_{L0}\mathbf{v}_0$ is the zero-load voltage.

Remark 1. Observe that (4) can be straightforwardly utilized in cases when a network features a mix of three-phase, two-phase, and single-phase buses. In particular, in that case, the vectors $\mathbf{v}$, $\mathbf{s}^Y$, and $\mathbf{w}$ collect their corresponding electrical quantities only for existing phases; the vector $\mathbf{s}^\Delta$ collects the existing phase-to-phase injections; and the matrix $\mathbf{H}$

[1]It was shown in [9], [17] that $\mathbf{Y}_{LL}$ is invertible for most practical cases of three-phase distribution networks.

contains rows that correspond to the existing phase-to-phase connections. For example, if a certain bus has only a single ab connection, it will only contain a row with $(1,-1,0)$ for that bus. In this case, $\mathbf{H}$ is $N^{\Delta} \times N^{phases}$ matrix, where N^{Δ} is the total number of phase-to-phase connections, and N^{phases} is the total number of phases in all the buses.

Remark 2. For exposition simplicity, the proposed method is outlined for the case of a constant-power load model. This is also motivated by recent optimization and control frameworks for distribution systems, where distributed energy resources as well as noncontrollable assets are (approximately) modeled as constant-PQ units [14], [15], [18]–[20]. However, the results in this paper can be naturally extended to a more general ZIP load model using a technique similar to [10].

III. Existence and Uniqueness

The fixed-point equation (4) leads to an iterative procedure wherein the vector of voltages is updated as:

$$\mathbf{v}^{(k+1)} = \mathbf{G}_{\mathbf{s}^Y \mathbf{s}^{\Delta}}(\mathbf{v}^{(k)}) \tag{5}$$

with $\mathbf{v}^{(0)}$ a given initialization point, k the iteration index, and $\mathbf{G}_{\mathbf{s}^Y \mathbf{s}^{\Delta}}(\cdot)$ defined in (4). Convergence of the iterative method (5) is analyzed next.

To this end, let $\mathbf{W} := \mathsf{diag}(\mathbf{w})$, and $\mathbf{L} := |\mathbf{H}|$ be the element-wise absolute value of the matrix $\mathbf{H}$. Also, for $\mathbf{s} := ((\mathbf{s}^Y)^{\mathsf{T}}, (\mathbf{s}^{\Delta})^{\mathsf{T}})^{\mathsf{T}} \in \mathbb{C}^{6N}$ define

$$\xi^Y(\mathbf{s}) := \left\| \mathbf{W}^{-1} \mathbf{Y}_{LL}^{-1} \mathbf{W}^{-1} \mathsf{diag}(\mathbf{s}^Y) \right\|_{\infty}, \tag{6a}$$

$$\xi^{\Delta}(\mathbf{s}) := \left\| \mathbf{W}^{-1} \mathbf{Y}_{LL}^{-1} \mathbf{H}^{\mathsf{T}} \mathsf{diag}(\mathbf{L}|\mathbf{w}|)^{-1} \mathsf{diag}(\mathbf{s}^{\Delta}) \right\|_{\infty}, \tag{6b}$$

$$\xi(\mathbf{s}) := \xi^Y(\mathbf{s}) + \xi^{\Delta}(\mathbf{s}), \tag{6c}$$

where $|\mathbf{w}|$ is the element-wise absolute value of the vector $\mathbf{w}$, and $\|\mathbf{A}\|_{\infty}$ is the induced ℓ_{∞}-norm of a complex matrix $\mathbf{A}$. Note that $\xi(\mathbf{s})$ defines a norm on $\mathbb{C}^{6N}$.

Lemma 1. *$\xi(\mathbf{s})$ is a norm on $\mathbb{C}^{6N}$.*

The proof of Lemma 1 as well as other technical results are deferred to the Appendix. Finally, let

$$\alpha(\mathbf{v}) := \min_j \frac{|(\mathbf{v})_j|}{|(\mathbf{w})_j|} \tag{7a}$$

$$\beta(\mathbf{v}) := \min_j \frac{|(\mathbf{H}\mathbf{v})_j|}{(\mathbf{L}|\mathbf{w}|)_j} \tag{7b}$$

$$\gamma(\mathbf{v}) := \min\{\alpha(\mathbf{v}),\, \beta(\mathbf{v})\} \tag{7c}$$

We next present our main result on the solution of the fixed-point equation defined by (4).

Theorem 1. *Let $\widehat{\mathbf{v}}$ be a given solution to the power-flow equations for a vector of power injections $\widehat{\mathbf{s}}$. Consider some other candidate vector of power injections $\mathbf{s}$, and assume that there exists a $\rho \in (0, \gamma(\widehat{\mathbf{v}}))$, such that*

$$\frac{\xi^Y(\mathbf{s}-\widehat{\mathbf{s}}) + \dfrac{\xi^Y(\widehat{\mathbf{s}})}{\alpha(\widehat{\mathbf{v}})}\rho}{\alpha(\widehat{\mathbf{v}}) - \rho} + \frac{\xi^{\Delta}(\mathbf{s}-\widehat{\mathbf{s}}) + \dfrac{\xi^{\Delta}(\widehat{\mathbf{s}})}{\beta(\widehat{\mathbf{v}})}\rho}{\beta(\widehat{\mathbf{v}}) - \rho} \leq \rho \tag{8}$$

and

$$\frac{\xi^Y(\mathbf{s})}{(\alpha(\widehat{\mathbf{v}}) - \rho)^2} + \frac{\xi^{\Delta}(\mathbf{s})}{(\beta(\widehat{\mathbf{v}}) - \rho)^2} < 1. \tag{9}$$

Then, there exists a unique solution $\mathbf{v}$ in

$$\mathcal{D}_{\rho}(\widehat{\mathbf{v}}) := \{\mathbf{v} :\, |(\mathbf{v})_j - (\widehat{\mathbf{v}})_j| \leq \rho |(\mathbf{w})_j|,\, j = 1 \ldots 3N\} \tag{10}$$

to the power-flow equations with power injection $\mathbf{s}$. Moreover, this solution can be reached by iteration (5) *initialized anywhere in $\mathcal{D}_{\rho}(\widehat{\mathbf{v}})$.*

The conditions of Theorem 1 may be computationally intensive as they require a parameter scanning to find a proper value for ρ. In the following, we sacrifice the tightness of the inequalities (8) and (9) to obtain the following more practical *explicit conditions*.

Theorem 2. *Let $\widehat{\mathbf{v}}$ be a given solution to the power-flow equations with power injection $\widehat{\mathbf{s}}$ satisfying:*

$$\xi(\widehat{\mathbf{s}}) < (\gamma(\widehat{\mathbf{v}}))^2. \tag{11}$$

Consider some other candidate power injections vector $\mathbf{s}$, and assume that

$$\xi(\mathbf{s}-\widehat{\mathbf{s}}) < \frac{1}{4}\left(\frac{(\gamma(\widehat{\mathbf{v}}))^2 - \xi(\widehat{\mathbf{s}})}{\gamma(\widehat{\mathbf{v}})}\right)^2. \tag{12}$$

Let

$$\rho^{\ddagger}(\widehat{\mathbf{v}}, \widehat{\mathbf{s}}) := \frac{1}{2}\left(\frac{(\gamma(\widehat{\mathbf{v}}))^2 - \xi(\widehat{\mathbf{s}})}{\gamma(\widehat{\mathbf{v}})}\right) \tag{13a}$$

$$\rho^{\dagger}(\widehat{\mathbf{v}}, \widehat{\mathbf{s}}, \mathbf{s}) := \rho^{\ddagger}(\widehat{\mathbf{v}}, \widehat{\mathbf{s}}) - \sqrt{(\rho^{\ddagger}(\widehat{\mathbf{v}}, \widehat{\mathbf{s}}))^2 - \xi(\mathbf{s}-\widehat{\mathbf{s}})} \tag{13b}$$

Then:

- *(i) There exists a unique load-flow solution $\mathbf{v}$ in $\mathcal{D}_{\rho}(\widehat{\mathbf{v}})$ defined in* (10) *with $\rho = \rho^{\ddagger}(\widehat{\mathbf{v}}, \widehat{\mathbf{s}})$.*
- *(ii) This solution can be reached by iteration* (5) *starting from anywhere in $\mathcal{D}_{\rho}(\widehat{\mathbf{v}})$ with $\rho = \rho^{\ddagger}(\widehat{\mathbf{v}}, \widehat{\mathbf{s}})$;*
- *(iii) The solution is located in $\mathcal{D}_{\rho}(\widehat{\mathbf{v}})$ with $\rho = \rho^{\dagger}(\widehat{\mathbf{v}}, \widehat{\mathbf{s}}, \mathbf{s})$.*

Note that if a solution to the load-flow problem $(\widehat{\mathbf{v}}, \widehat{\mathbf{s}})$ is not always available, one can simply set $\widehat{\mathbf{v}} = \mathbf{w}$ and $\widehat{\mathbf{s}} = 0$ (with $\mathbf{w}$ the zero-load voltage profile); see, e.g., [9], [10].

IV. Linear Models

In this section, we develop two methods to obtain approximate representations of the AC power-flow equations (1), wherein the net injected powers and voltages are related through an approximate linear relationship. The first method is based on the first-order Taylor (FOT) expansion of the load-flow solution around a given point. FOT is therefore the best local linear approximator. The second method is based on a single iteration of the fixed-point iteration (5) and it is hereafter referred to as fixed-point linearization (FPL).

Let $\mathbf{p}^Y := \Re\{\mathbf{s}^Y\}$, $\mathbf{q}^Y := \Im\{\mathbf{s}^Y\}$, $\mathbf{p}^{\Delta} := \Re\{\mathbf{s}^{\Delta}\}$, $\mathbf{q}^{\Delta} := \Im\{\mathbf{s}^{\Delta}\}$, $\mathbf{x}^Y := ((\mathbf{p}^Y)^{\mathsf{T}}, (\mathbf{q}^Y)^{\mathsf{T}})^{\mathsf{T}}$, and $\mathbf{x}^{\Delta} := ((\mathbf{p}^{\Delta})^{\mathsf{T}}, (\mathbf{q}^{\Delta})^{\mathsf{T}})^{\mathsf{T}}$ collect the active and reactive power injections. Also, let $|\mathbf{v}|$ collect the voltage magnitudes. Our goal is to derive linear approximations to (1) in the form

$$\widetilde{\mathbf{v}} = \mathbf{M}^Y \mathbf{x}^Y + \mathbf{M}^{\Delta} \mathbf{x}^{\Delta} + \mathbf{a}, \tag{14a}$$

$$|\widetilde{\mathbf{v}}| = \mathbf{K}^Y \mathbf{x}^Y + \mathbf{K}^{\Delta} \mathbf{x}^{\Delta} + \mathbf{b}, \tag{14b}$$

for some matrices $\mathbf{M}^Y, \mathbf{M}^{\Delta} \in \mathbb{C}^{3N \times 6N}$, $\mathbf{K}^Y, \mathbf{K}^{\Delta} \in \mathbb{R}^{3N \times 6N}$, and vectors $\mathbf{a} \in \mathbb{C}^{3N}, \mathbf{b} \in \mathbb{R}^{3N}$.

A. First-Order Taylor (FOT) Method

To obtain (14a), linearize (1) around a given operating point $\widehat{\mathbf{v}}, \widehat{\mathbf{x}}^Y, \widehat{\mathbf{x}}^\Delta$, by computing $\mathbf{M}^Y$ and $\mathbf{M}^\Delta$ as follows:

$$\mathbf{M}^Y := \frac{\partial \mathbf{v}}{\partial \mathbf{x}^Y}, \quad \mathbf{M}^\Delta := \frac{\partial \mathbf{v}}{\partial \mathbf{x}^\Delta}$$

and by setting $\mathbf{a} := \widehat{\mathbf{v}} - \mathbf{M}^Y \widehat{\mathbf{x}}^Y - \mathbf{M}^\Delta \widehat{\mathbf{x}}^\Delta$. To this end, plug (1c) into (1a), and take partial derivatives of (1a) and (1b) with respect to $\mathbf{x}^Y$ and $\mathbf{x}^\Delta$:

$$\begin{aligned}
&\mathsf{diag}\left(\mathbf{H}^\mathsf{T}\overline{\mathbf{i}^\Delta}\right)\frac{\partial \mathbf{v}}{\partial \mathbf{x}^Y} + \mathsf{diag}(\mathbf{v})\mathbf{H}^\mathsf{T}\frac{\partial \overline{\mathbf{i}^\Delta}}{\partial \mathbf{x}^Y} + \mathbf{U} \\
&= \mathsf{diag}(\mathbf{v})\overline{\mathbf{Y}}_{LL}\frac{\partial \overline{\mathbf{v}}}{\partial \mathbf{x}^Y} + \mathsf{diag}(\overline{\mathbf{Y}}_{L0}\overline{\mathbf{v}}_0 + \overline{\mathbf{Y}}_{LL}\overline{\mathbf{v}})\frac{\partial \mathbf{v}}{\partial \mathbf{x}^Y}, \quad (15a)\\
&\mathbf{0} = \mathsf{diag}\left(\mathbf{H}\mathbf{v}\right)\frac{\partial \overline{\mathbf{i}^\Delta}}{\partial \mathbf{x}^Y} + \mathsf{diag}(\overline{\mathbf{i}^\Delta})\mathbf{H}\frac{\partial \mathbf{v}}{\partial \mathbf{x}^Y}, \quad (15b)\\
&\mathsf{diag}\left(\mathbf{H}^\mathsf{T}\overline{\mathbf{i}^\Delta}\right)\frac{\partial \mathbf{v}}{\partial \mathbf{x}^\Delta} + \mathsf{diag}(\mathbf{v})\mathbf{H}^\mathsf{T}\frac{\partial \overline{\mathbf{i}^\Delta}}{\partial \mathbf{x}^\Delta} \\
&= \mathsf{diag}(\mathbf{v})\overline{\mathbf{Y}}_{LL}\frac{\partial \overline{\mathbf{v}}}{\partial \mathbf{x}^\Delta} + \mathsf{diag}(\overline{\mathbf{Y}}_{L0}\overline{\mathbf{v}}_0 + \overline{\mathbf{Y}}_{LL}\overline{\mathbf{v}})\frac{\partial \mathbf{v}}{\partial \mathbf{x}^\Delta}, \quad (15c)\\
&\mathbf{U} = \mathsf{diag}\left(\mathbf{H}\mathbf{v}\right)\frac{\partial \overline{\mathbf{i}^\Delta}}{\partial \mathbf{x}^\Delta} + \mathsf{diag}(\overline{\mathbf{i}^\Delta})\mathbf{H}\frac{\partial \mathbf{v}}{\partial \mathbf{x}^\Delta}, \quad (15d)
\end{aligned}$$

where $\mathbf{U} := (\mathbf{I}, \jmath\mathbf{I}) \in \mathbb{C}^{3N\times 6N}$ and $\mathbf{I} \in \mathbb{R}^{3N\times 3N}$ is the identity matrix. In this set of equations, set $\mathbf{v} = \widehat{\mathbf{v}}$ and $\overline{\mathbf{i}^\Delta} = \mathsf{diag}(\mathbf{H}\widehat{\mathbf{v}})^{-1}\overline{\mathbf{s}^\Delta}$; the unknowns are the matrices $\frac{\partial \mathbf{v}}{\partial \mathbf{x}^Y}, \frac{\partial \overline{\mathbf{i}^\Delta}}{\partial \mathbf{x}^Y}, \frac{\partial \mathbf{v}}{\partial \mathbf{x}^\Delta}, \frac{\partial \overline{\mathbf{i}^\Delta}}{\partial \mathbf{x}^\Delta} \in \mathbb{C}^{3N\times 6N}$.

Observe that, in rectangular coordinates, (15) is a set of *linear* equations with the same number, $(12N)^2$, of real-valued equations and variables. We next give conditions under which the system of equations (15) has a unique solution. The power-flow equations (1) define an explicit mapping $\mathbf{y} \to \mathbf{x}$ with $\mathbf{x} := \left((\mathbf{x}^Y)^\mathsf{T}, (\mathbf{x}^\Delta)^\mathsf{T}\right)^\mathsf{T}$ and $\mathbf{y} := \left(\Re\{\mathbf{v}\}^\mathsf{T}, \Im\{\mathbf{v}\}^\mathsf{T}, \Re\{\mathbf{i}^\Delta\}^\mathsf{T}, \Im\{\mathbf{i}^\Delta\}^\mathsf{T}\right)^\mathsf{T}$, $i, j = 1, \ldots, 12N$. Let $\mathbf{J}$ be the Jacobian matrix of this mapping, i.e., $(\mathbf{J})_{ij} = \frac{\partial(\mathbf{x})_i}{\partial(\mathbf{y})_j}$,

Theorem 3. *Let $(\widehat{\mathbf{v}}, \widehat{\mathbf{s}})$ be a given operating point. Suppose that either of the following two conditions hold: (i) the Jacobian $\mathbf{J}$ is non-singular, or (ii) condition* (11) *is satisfied. Then the system* (15) *has a unique solution.*

To obtain the linear model for the voltage magnitudes $|\mathbf{v}|$ in (14b), we leverage the following derivation rule:

$$\frac{\partial |f(x)|}{\partial x} = \frac{1}{|f(x)|}\Re\left\{\overline{f(x)}\frac{\partial f(x)}{\partial x}\right\}.$$

It then follows that matrices $\mathbf{K}^Y$ and $\mathbf{K}^\Delta$ are given by:

$$\begin{aligned}
\mathbf{K}^Y &:= \frac{\partial |\mathbf{v}|}{\partial \mathbf{x}^Y} = \mathsf{diag}(|\widehat{\mathbf{v}}|)^{-1}\Re\left\{\mathsf{diag}(\overline{\widehat{\mathbf{v}}})\mathbf{M}^Y\right\}, \quad (16a)\\
\mathbf{K}^\Delta &:= \frac{\partial |\mathbf{v}|}{\partial \mathbf{x}^\Delta} = \mathsf{diag}(|\widehat{\mathbf{v}}|)^{-1}\Re\left\{\mathsf{diag}(\overline{\widehat{\mathbf{v}}})\mathbf{M}^\Delta\right\}, \quad (16b)\\
\mathbf{b} &:= |\widehat{\mathbf{v}}| - \mathbf{K}^Y\widehat{\mathbf{x}}^Y - \mathbf{K}^\Delta\widehat{\mathbf{x}}^\Delta. \quad (16c)
\end{aligned}$$

B. Fixed-Point Linearization (FPL) Method

Let $\widehat{\mathbf{v}}, \widehat{\mathbf{s}}^Y, \widehat{\mathbf{s}}^\Delta$ be a given solution to the fixed point equation (4). Consider the first iteration of the fixed-point method (5) initialized at $\widehat{\mathbf{v}}$:

$$\widetilde{\mathbf{v}} = \mathbf{w} + \mathbf{Y}_{LL}^{-1}\left(\mathsf{diag}(\overline{\widehat{\mathbf{v}}})^{-1}\overline{\mathbf{s}^Y} + \mathbf{H}^\mathsf{T}\mathsf{diag}\left(\mathbf{H}\widehat{\mathbf{v}}\right)^{-1}\overline{\mathbf{s}^\Delta}\right) \quad (17)$$

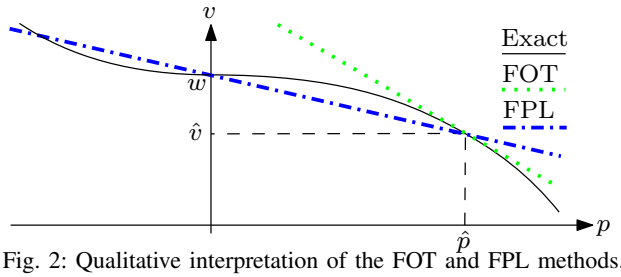

Fig. 2: Qualitative interpretation of the FOT and FPL methods.

which gives an *explicit* linear model (14a) provided by

$$\begin{aligned}
\mathbf{M}^Y &:= \left(\mathbf{Y}_{LL}^{-1}\mathsf{diag}(\overline{\widehat{\mathbf{v}}})^{-1}, -\jmath\mathbf{Y}_{LL}^{-1}\mathsf{diag}(\overline{\widehat{\mathbf{v}}})^{-1}\right)\\
\mathbf{M}^\Delta &:= \left(\mathbf{Y}_{LL}^{-1}\mathbf{H}^\mathsf{T}\mathsf{diag}\left(\mathbf{H}\overline{\widehat{\mathbf{v}}}\right)^{-1}, -\jmath\mathbf{Y}_{LL}^{-1}\mathbf{H}^\mathsf{T}\mathsf{diag}\left(\mathbf{H}\overline{\widehat{\mathbf{v}}}\right)^{-1}\right)
\end{aligned}$$

and $\mathbf{a} = \mathbf{w}$. The model (14b) can be then obtained using (16) as before. We next provide an upper bound for the linearization error of the FPL method.

Theorem 4. *Suppose that $(\widehat{\mathbf{v}}, \widehat{\mathbf{s}})$ satisfy condition* (11)*. Let $\mathbf{s}$ be the vector of power injections that satisfies* (12)*, and let $\mathbf{v} \in \mathcal{D}_{\rho^\dagger}(\widehat{\mathbf{v}})$ be the corresponding unique load-flow solution as asserted by Theorem 2. Then the approximation error of* (17) *can be upper bounded by*

$$\|\widetilde{\mathbf{v}} - \mathbf{v}\|_\infty \le q\rho^\dagger\|\mathbf{w}\|_\infty \quad (18)$$

where

$$q := \frac{\xi^Y(\mathbf{s})}{(\alpha(\widehat{\mathbf{v}}) - \rho^\dagger)^2} + \frac{\xi^\Delta(\mathbf{s})}{(\beta(\widehat{\mathbf{v}}) - \rho^\dagger)^2} < 1.$$

The difference between the two linearization methods is conceptually illustrated in Figure 2. The fixed-point linearization method can be viewed as an *interpolation* method between two load-flow solutions: $(\mathbf{w}, \mathbf{0})$ and $(\widehat{\mathbf{v}}, \widehat{\mathbf{s}})$. On the other hand, the FOT yields the tangent plane of the power-flow manifold at the current linearization point.

Some qualitative comparison between the FOT and FPL methods follows (a numerical comparison is provided shortly in Section V). The FOT method provides the best local linear approximator, and hence it is expected to provide the best approximation accuracy around the linearization point. However, the main downside of the FOT method is its computational complexity. Indeed, solving $(12N)^2$ equations with $(12N)^2$ variables might not be feasible for large N (i.e., large networks). On the other hand, the FPL method is computationally affordable as it requires only elementary vector-matrix multiplications (provided that $\mathbf{Y}_{LL}^{-1}$ is precomputed in advance). Moreover, if global behaviour is of interest, it can also provide a better approximation (cf. Figure 2).

V. Numerical Evaluation

In this section, we evaluate numerically the proposed conditions on the existence and uniqueness of load-flow solutions, and we assess the approximation error of the FOT and FPL methods. Two IEEE benchmark networks are used to perform the experiments: the 37-node feeder and the 123-node feeder [21]. To assess the performance for different generation/loading conditions, we perform a *continuation analysis*:

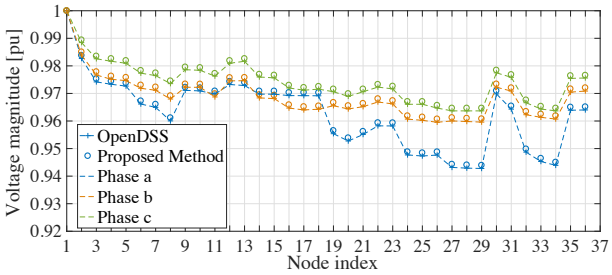

Fig. 3: Comparison to OpenDSS solution.

TABLE I: Additional Power Sources in 37-Bus Feeder

Bus	Phase a (p.u.)	Phase b (p.u.)	Phase c (p.u.)
701	-0.05-0.02$\jmath$	-0.05-0.02$\jmath$	-0.05-0.02$\jmath$
730	-0.03-0.01$\jmath$	0	0
720	0	-0.04-0.02$\jmath$	0
742	0.04	0	0.04
735	0.03+0.01$\jmath$	0.03+0.01$\jmath$	0.03+0.01$\jmath$
737	-0.02-0.01$\jmath$	-0.02-0.01$\jmath$	-0.02-0.01$\jmath$

given a reference vector of power injections $\mathbf{s}^{\text{ref}}$, we evaluate the conditions and the approximation error of the linear models by setting $\mathbf{s} = \kappa \mathbf{s}^{\text{ref}}$, for $\kappa \in \mathbb{R}$.

A. IEEE 37-Bus Feeder

Similar to prior works [14], [15], [18]–[20], we first translate all constant-current and constant-impedance sources in the IEEE data set into constant-power sources.

1) Original Injections Data: In the original IEEE data set, all sources are delta-connected. Denote this reference power injection vector by $\mathbf{s}^{\text{ref}}$, and let the target power injection be $\mathbf{s} = \kappa \mathbf{s}^{\text{ref}}$ with κ as a nonnegative real number. As there are no mixed wye and delta sources, the conditions on the existence and uniqueness of the load-flow solutions in [10] are also applicable. For comparison, we take the diagonal matrix $\mathbf{\Lambda}$ in [10] to be $\mathbf{W}$, as suggested there. In Figure 4a, we plot five power intervals in p.u. Interval 1 contains the power injection $\mathbf{s}$ that satisfies the four conditions in [10]; Interval 2 (resp. 3) shows the injections $\mathbf{s}$ that satisfy the conditions in Theorem 1 (resp. Theorem 2) with $(\widehat{\mathbf{v}}, \widehat{\mathbf{s}}) = (\mathbf{w}, \mathbf{0})$. For the rightmost power $\mathbf{s}^{(1)} = 3.45\mathbf{s}^{\text{ref}}$, we compute the load-flow solution using iteration (5). By choosing this solution and $\mathbf{s}^{(1)}$ as the new $(\widehat{\mathbf{v}}, \widehat{\mathbf{s}})$, we obtain Interval 4 (resp. 5) via Theorem 1 (resp. Theorem 2).

Numerically, Intervals 1,2, and 3 are almost the same. However, the complexity of computing Interval 3 is much smaller because of the low computational complexity of verifying conditions (11) and (12). More importantly, Intervals 4 and 5 contain points that are not guaranteed to have the unique solution using the method in [10] – compare to Interval 1. Thus, the proposed method allows for certifying the existence and uniqueness of the load-flow solution for a wider range of power injections.

2) Mixed Delta and Wye Connections: One of the key advantages of the proposed method is the ability to handle buses with both delta- and wye-connected sources/loads. To this end, we add wye-connected elements to some buses of the feeder, where delta-connected loads are already present. The data is provided in Table I, with a positive sign meaning power generation. As mentioned, the only freely-available power-flow solver that can address the case of mixed wye and delta connections is part of the OpenDSS platform [13]. We thus first compare the solution produced by iteration (5) initialized at $\mathbf{w}$ to that of OpenDSS. The two load-flow solutions are shown in Figure 3: the achieved voltage profiles match (within given numerical accuracy).

TABLE II: Additional Power Sources in 123-Bus Feeder

Bus	Type	Phase-Phase ab / Phase a (p.u.)	Phase-Phase bc / Phase b (p.u.)	Phase-Phase ca / Phase c (p.u.)
1	delta	-0.03-0.01$\jmath$	-0.03-0.01$\jmath$	-0.03-0.01$\jmath$
35	wye	-0.02	-0.02	-0.02
76	wye	0.04+0.01$\jmath$	0.04+0.01$\jmath$	0.04+0.01$\jmath$
99	delta	-0.02-0.01$\jmath$	-0.02-0.01$\jmath$	-0.02-0.01$\jmath$

Next, we evaluate the conditions provided by Theorems 1 and 2 using this modified reference power injections vector, as shown in Figure 4b. Similarly to Figure 4a, Interval 1 (resp. 2) includes power injections $\mathbf{s}$ fulfilling conditions in Theorem 1 (resp. 2) with $(\widehat{\mathbf{v}}, \widehat{\mathbf{s}}) = (\mathbf{w}, \mathbf{0})$. Then, we apply iteration (5) to compute the load-flow solution to power injection $\mathbf{s}^{(1)} = 1.23\mathbf{s}^{\text{ref}}$ located rightmost on Interval 1, and use Theorem 1 (resp. 2) to obtain Interval 3 (resp. 4) using this new $(\widehat{\mathbf{v}}, \widehat{\mathbf{s}})$. As shown, the interval obtained by Theorem 1 is bigger than that of Theorem 2. This comes at the expense of the computational complexity of evaluating the condition of Theorem 1.

Finally, we evaluate the performance of the two linearization methods proposed in Section IV. Figure 4c shows the results of the continuation analysis for relative errors for both linear models using $\kappa \in [-1.5, 1.5]$. As shown, both linear models behave well with relative errors below 1%. Moreover, the FOT method has a smaller error around the linearization point whereas the FPL method provides for a more global approximation. This corroborates the intuitive illustration in Figure 2. For linear approximations of voltage magnitudes, the errors are at a similar level; hence, for brevity, we do not show them explicitly.

B. IEEE 123-Bus Feeder

In this section, we consider a larger multiphase network with unbalanced one-, two-, and three-phase sources/loads. As mentioned in Remark 1, we first delete in matrix $\mathbf{H}$ the rows that correspond to the lacking phase-to-phase connections and the columns that correspond to the lacking phases.

The results of the continuation analysis for conditions' evaluation are shown in Figures 5a and 5b, with the same interpretation of the intervals as in Figures 4a and 4b. To perform the experiment with mixed delta-wye connections (Figure 5b), additional power sources/loads were added to the network, as shown in Table II.

Finally, in Figure 5c, we show the results of the continuation analysis for the relative errors for both linear models using $\kappa \in [-1.5, 1.5]$. Clearly, the errors vary in a way that is similar to the illustration in Figure 2. In other words, the FPL method provides not only a high computational efficiency but also a better global performance for large distribution networks.

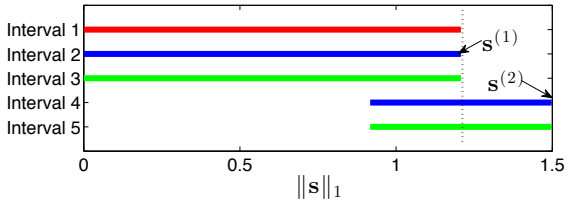

(a) Original injections data. Power intervals (in p.u.) that satisfy conditions on the existence and uniqueness of the load-flow solutions (Intervals 2, 3, 4, and 5) and comparison to the interval obtained by [10] (Interval 1).

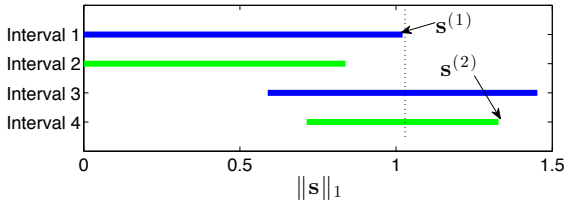

(b) Mixed delta and wye sources. Power intervals (in p.u.) that satisfy conditions on the existence and uniqueness of the load-flow solutions.

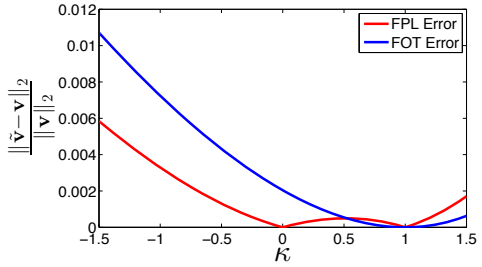

(c) Relative errors in complex load-flow solutions for FOT and FPL methods.

Fig. 4: Continuation analysis for the 37-bus feeder.

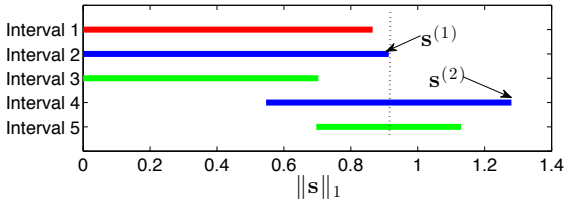

(a) Original injections data. Power intervals (in p.u.) that satisfy conditions on the existence and uniqueness of the load-flow solutions (Intervals 2, 3, 4, and 5) and comparison to the interval obtained by [10] (Interval 1).

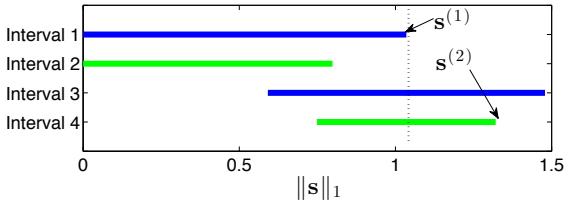

(b) Mixed delta and wye sources. Power intervals (in p.u.) that satisfy conditions on the existence and uniqueness of the load-flow solutions.

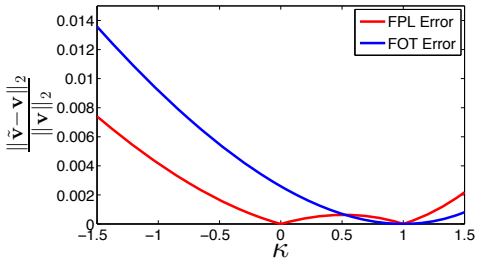

(c) Relative errors in complex load-flow solutions for FOT and FPL methods.

Fig. 5: Continuation analysis for the 123-bus feeder.

VI. Conclusion

The paper proposed a load-flow algorithm for general multiphase distribution systems. Explicit conditions for the existence and uniqueness of the load-flow solutions we derived, and conditions that guarantee the convergence of the load-flow algorithm to the unique power-flow solution were analytically established. Linear load-flow models were proposed and their approximation accuracy was analyzed. Theoretical results were corroborated through numerical experiments on IEEE test feeders.

Appendix

A. Proof of Lemma 1

We need to show the three norm axioms. Trivially, note that $\xi(a\mathbf{s}) = |a|\xi(\mathbf{s})$ for any $a \in \mathbb{C}$. Next, the triangle inequality holds because

$$\begin{aligned}
\xi(\mathbf{s}+\mathbf{s}') &= \left\|\mathbf{W}^{-1}\mathbf{Y}_{LL}^{-1}\mathbf{W}^{-1}\mathsf{diag}(\mathbf{s}^{Y}+\mathbf{s}'^{Y})\right\|_\infty \\
&\quad + \left\|\mathbf{W}^{-1}\mathbf{Y}_{LL}^{-1}\mathbf{H}^{\mathsf{T}}\mathsf{diag}(\mathbf{L}|\mathbf{w}|)^{-1}\mathsf{diag}(\mathbf{s}^{\Delta}+\mathbf{s}'^{\Delta})\right\|_\infty \\
&= \left\|\mathbf{W}^{-1}\mathbf{Y}_{LL}^{-1}\mathbf{W}^{-1}\mathsf{diag}(\mathbf{s}^{Y}) + \mathbf{W}^{-1}\mathbf{Y}_{LL}^{-1}\mathbf{W}^{-1}\mathsf{diag}(\mathbf{s}'^{Y})\right\|_\infty \\
&\quad + \Big\|\mathbf{W}^{-1}\mathbf{Y}_{LL}^{-1}\mathbf{H}^{\mathsf{T}}\mathsf{diag}(\mathbf{L}|\mathbf{w}|)^{-1}\mathsf{diag}(\mathbf{s}^{\Delta}) + \\
&\qquad \mathbf{W}^{-1}\mathbf{Y}_{LL}^{-1}\mathbf{H}^{\mathsf{T}}\mathsf{diag}(\mathbf{L}|\mathbf{w}|)^{-1}\mathsf{diag}(\mathbf{s}'^{\Delta})\Big\|_\infty \\
&\leq \xi^{Y}(\mathbf{s}) + \xi^{Y}(\mathbf{s}') + \xi^{\Delta}(\mathbf{s}) + \xi^{\Delta}(\mathbf{s}') = \xi(\mathbf{s}) + \xi(\mathbf{s}'),
\end{aligned}$$

where the inequality follows by the triangle inequality for the induced matrix norm. Finally, if $\xi(\mathbf{s}) = 0$, it necessarily holds that $\mathbf{W}^{-1}\mathbf{Y}_{LL}^{-1}\mathbf{W}^{-1}\mathsf{diag}(\mathbf{s}^{Y})$ and $\mathbf{W}^{-1}\mathbf{Y}_{LL}^{-1}\mathbf{H}^{\mathsf{T}}\mathsf{diag}(\mathbf{L}|\mathbf{w}|)^{-1}\mathsf{diag}(\mathbf{s}^{\Delta})$ are zero matrices. This necessarily implies that $\mathbf{s}^{Y}$ and $\mathbf{s}^{\Delta}$ are zero vectors.

B. Proof of Theorem 1

For the purpose of the proof, we find it convenient to re-parametrize using $\mathbf{u} := \mathbf{W}^{-1}\mathbf{v}$. Then, (4) is equivalent to

$$\begin{aligned}
\mathbf{u} = \widetilde{\mathbf{G}}_{\mathbf{s}^{Y}\mathbf{s}^{\Delta}}(\mathbf{u}) &= \mathbf{1} + \mathbf{W}^{-1}\mathbf{Y}_{LL}^{-1}\overline{\mathbf{W}}^{-1}\mathsf{diag}(\overline{\mathbf{u}})^{-1}\overline{\mathbf{s}^{Y}} \\
&\quad + \mathbf{W}^{-1}\mathbf{Y}_{LL}^{-1}\mathbf{H}^{\mathsf{T}}\mathsf{diag}\left(\mathbf{H}\overline{\mathbf{W}}\overline{\mathbf{u}}\right)^{-1}\overline{\mathbf{s}^{\Delta}}. \qquad (19)
\end{aligned}$$

As $\mathbf{W}$ defines an invertible relationship between $\mathbf{v}$ and $\mathbf{u}$, we next focus on the solution properties of (19). By the Banach fixed-point theorem, what we need to show is that $\widetilde{\mathbf{G}}_{\mathbf{s}^{Y}\mathbf{s}^{\Delta}}(\mathbf{u})$ is a self-mapping and contraction mapping on

$$\widetilde{\mathcal{D}}_\rho(\widehat{\mathbf{u}}) := \{\mathbf{u} : |(\mathbf{u})_j - (\widehat{\mathbf{u}})_j| \leq \rho,\ j = 1\dots 3N\} \qquad (20)$$

for some $\rho \in (0, \gamma(\widehat{\mathbf{v}}))$ that satisfies (8) and (9).

1) Proof of Self-Mapping: The goal here is to show that, for $\rho \in (0, \gamma(\widehat{\mathbf{v}}))$ fulfilling (8), $\|\mathbf{u}^{(k)} - \widehat{\mathbf{u}}\|_\infty \leq \rho$ leads to $\|\mathbf{u}^{(k+1)} - \widehat{\mathbf{u}}\|_\infty \leq \rho$.

By definition, we have

$$\begin{aligned}
&\mathbf{u}^{(k+1)}-\widehat{\mathbf{u}}\\
&=\mathbf{W}^{-1}\mathbf{Y}_{LL}^{-1}\overline{\mathbf{W}}^{-1}\left(\mathsf{diag}(\overline{\mathbf{u}}^{(k)})^{-1}\overline{\mathbf{s}^{Y}}-\mathsf{diag}(\widehat{\mathbf{u}})^{-1}\widehat{\mathbf{s}^{Y}}\right)\\
&+\mathbf{W}^{-1}\mathbf{Y}_{LL}^{-1}\mathbf{H}^{T}\left(\mathsf{diag}(\mathbf{H}\overline{\mathbf{W}}\overline{\mathbf{u}}^{(k)})^{-1}\overline{\mathbf{s}^{\Delta}}-\mathsf{diag}(\mathbf{H}\overline{\mathbf{W}}\widehat{\mathbf{u}})^{-1}\widehat{\mathbf{s}^{\Delta}}\right)\\
&=\mathbf{W}^{-1}\mathbf{Y}_{LL}^{-1}\overline{\mathbf{W}}^{-1}\left(\mathsf{diag}(\overline{\mathbf{u}}^{(k)})^{-1}\overline{\mathbf{s}^{Y}}-\mathsf{diag}(\overline{\mathbf{u}}^{(k)})^{-1}\widehat{\mathbf{s}^{Y}}\right)\\
&+\mathbf{W}^{-1}\mathbf{Y}_{LL}^{-1}\overline{\mathbf{W}}^{-1}\left(\mathsf{diag}(\overline{\mathbf{u}}^{(k)})^{-1}\widehat{\mathbf{s}^{Y}}-\mathsf{diag}(\widehat{\mathbf{u}})^{-1}\widehat{\mathbf{s}^{Y}}\right)\\
&+\mathbf{W}^{-1}\mathbf{Y}_{LL}^{-1}\mathbf{H}^{T}\left(\mathsf{diag}(\mathbf{H}\overline{\mathbf{W}}\overline{\mathbf{u}}^{(k)})^{-1}\overline{\mathbf{s}^{\Delta}}-\mathsf{diag}(\mathbf{H}\overline{\mathbf{W}}\overline{\mathbf{u}}^{(k)})^{-1}\widehat{\mathbf{s}^{\Delta}}\right)\\
&+\mathbf{W}^{-1}\mathbf{Y}_{LL}^{-1}\mathbf{H}^{T}\left(\mathsf{diag}(\mathbf{H}\overline{\mathbf{W}}\overline{\mathbf{u}}^{(k)})^{-1}\widehat{\mathbf{s}^{\Delta}}-\mathsf{diag}(\mathbf{H}\overline{\mathbf{W}}\widehat{\mathbf{u}})^{-1}\widehat{\mathbf{s}^{\Delta}}\right). \quad (21)
\end{aligned}$$

We can rearrange the right-hand side of (21) as follows. For example, for the second term, we have

$$\begin{aligned}
&\mathbf{W}^{-1}\mathbf{Y}_{LL}^{-1}\overline{\mathbf{W}}^{-1}\left(\mathsf{diag}(\overline{\mathbf{u}}^{(k)})^{-1}\widehat{\mathbf{s}^{Y}}-\mathsf{diag}(\widehat{\mathbf{u}})^{-1}\widehat{\mathbf{s}^{Y}}\right)\\
&=-\mathbf{W}^{-1}\mathbf{Y}_{LL}^{-1}\overline{\mathbf{W}}^{-1}\mathsf{diag}(\widehat{\mathbf{s}^{Y}})\begin{bmatrix}\frac{(\overline{\mathbf{u}}^{(k)})_1-(\widehat{\mathbf{u}})_1}{(\overline{\mathbf{u}}^{(k)})_1(\widehat{\mathbf{u}})_1}\cdots\frac{(\overline{\mathbf{u}}^{(k)})_{3N}-(\widehat{\mathbf{u}})_{3N}}{(\overline{\mathbf{u}}^{(k)})_{3N}(\widehat{\mathbf{u}})_{3N}}\end{bmatrix}^{\mathsf{T}} \quad (22)
\end{aligned}$$

Similar rearrangements can be applied to the remaining terms in (21). Therefore, by triangular inequality, the definition of the induced matrix norm, and definition (6), it holds that

$$\begin{aligned}
&\|\mathbf{u}^{(k+1)}-\widehat{\mathbf{u}}\|_\infty\le\xi^{Y}(\mathbf{s}-\widehat{\mathbf{s}})\max_{j\in\{1,\dots,3N\}}\left(1/|(\mathbf{u}^{(k)})_j|\right)\\
&+\xi^{Y}(\widehat{\mathbf{s}})\max_{j\in\{1,\dots,3N\}}\left(|(\mathbf{u}^{(k)})_j-(\widehat{\mathbf{u}})_j|/[|(\mathbf{u}^{(k)})_j||(\widehat{\mathbf{u}})_j|]\right)\\
&+\xi^{\Delta}(\mathbf{s}-\widehat{\mathbf{s}})\max_{j\in\{1,\dots,3N\}}\left(1\Big/\frac{|(\mathbf{H}\mathbf{W}\mathbf{u}^{(k)})_j|}{(\mathbf{L}|\mathbf{w}|)_j}\right)\\
&+\xi^{\Delta}(\widehat{\mathbf{s}})\max_{j\in\{1,\dots,3N\}}\frac{|(\mathbf{H}\mathbf{W}\mathbf{u}^{(k)})_j-(\mathbf{H}\mathbf{W}\widehat{\mathbf{u}})_j|/(\mathbf{L}|\mathbf{w}|)_j}{\frac{|(\mathbf{H}\mathbf{W}\mathbf{u}^{(k)})_j|}{(\mathbf{L}|\mathbf{w}|)_j}\frac{|(\mathbf{H}\mathbf{W}\widehat{\mathbf{u}})_j|}{(\mathbf{L}|\mathbf{w}|)_j}}. \quad (23)
\end{aligned}$$

Observe that the following is true for any $j\in\{1,...,3N\}$ whenever $\|\mathbf{u}^{(k)}-\widehat{\mathbf{u}}\|\le\rho$:

$$|(\mathbf{u}^{(k)})_j|\ge|(\widehat{\mathbf{u}})_j|-|(\mathbf{u}^{(k)})_j-(\widehat{\mathbf{u}})_j|\ge\alpha(\widehat{\mathbf{v}})-\rho \quad (24a)$$

$$|(\mathbf{H}\mathbf{W}\mathbf{u}^{(k)})_j-(\mathbf{H}\mathbf{W}\widehat{\mathbf{u}})_j|\le(\mathbf{L}|\mathbf{w}|)_j\rho \quad (24b)$$

$$|(\mathbf{H}\mathbf{W}\mathbf{u}^{(k)})_j|\ge(\beta(\widehat{\mathbf{v}})-\rho)(\mathbf{L}|\mathbf{w}|)_j, \quad (24c)$$

where $\alpha(\cdot)$ and $\beta(\cdot)$ are defined in (7). In details, (24b) holds because

$$\begin{aligned}
&|(\mathbf{H}\mathbf{W}\mathbf{u}^{(k)})_j-(\mathbf{H}\mathbf{W}\widehat{\mathbf{u}})_j|\\
&=\left|\left((\mathbf{w})_\ell(\mathbf{u}^{(k)})_\ell-(\mathbf{w})_{\ell'}(\mathbf{u}^{(k)})_{\ell'}\right)-((\mathbf{w})_\ell(\widehat{\mathbf{u}})_\ell-(\mathbf{w})_{\ell'}(\widehat{\mathbf{u}})_{\ell'})\right|\\
&\le|(\mathbf{w})_\ell|\left|(\mathbf{u}^{(k)})_\ell-(\widehat{\mathbf{u}})_\ell\right|+|(\mathbf{w})_{\ell'}|\left|(\mathbf{u}^{(k)})_{\ell'}-(\widehat{\mathbf{u}})_{\ell'}\right|\\
&\le(|(\mathbf{w})_\ell|+|(\mathbf{w})_{\ell'}|)\,\|\mathbf{u}^{(k)}-\widehat{\mathbf{u}}\|_\infty\le(\mathbf{L}|\mathbf{w}|)_j\rho \quad (25)
\end{aligned}$$

for some ℓ,ℓ' in $\{1,...,3N\}$, and (24c) holds because

$$\begin{aligned}
&|(\mathbf{H}\mathbf{W}\mathbf{u}^{(k)})_j|\ge|(\mathbf{H}\mathbf{W}\widehat{\mathbf{u}})_j|-|(\mathbf{H}\mathbf{W}\mathbf{u}^{(k)})_j-(\mathbf{H}\mathbf{W}\widehat{\mathbf{u}})_j|\\
&\ge(\beta(\widehat{\mathbf{v}})-\rho)(\mathbf{L}|\mathbf{w}|)_j. \quad (26)
\end{aligned}$$

In this way, for $\rho\in(0,\gamma(\widehat{\mathbf{v}}))$, we obtain

$$\begin{aligned}
&\|\mathbf{u}^{(k+1)}-\widehat{\mathbf{u}}\|_\infty\\
&\le\frac{\xi^{Y}(\mathbf{s}-\widehat{\mathbf{s}})+\rho\xi^{Y}(\widehat{\mathbf{s}})/\alpha(\widehat{\mathbf{v}})}{\alpha(\widehat{\mathbf{v}})-\rho}+\frac{\xi^{\Delta}(\mathbf{s}-\widehat{\mathbf{s}})+\rho\xi^{\Delta}(\widehat{\mathbf{s}})/\beta(\widehat{\mathbf{v}})}{\beta(\widehat{\mathbf{v}})-\rho}. \quad (27)
\end{aligned}$$

This implies that $\|\mathbf{u}^{(k)}-\widehat{\mathbf{u}}\|_\infty\le\rho$ gives $\|\mathbf{u}^{(k+1)}-\widehat{\mathbf{u}}\|_\infty\le\rho$ for $\rho\in(0,\gamma(\widehat{\mathbf{v}}))$ fulfilling (8), and hence completes the proof.

2) Proof of Contraction: In this part, assuming there is a $\rho\in(0,\gamma(\widehat{\mathbf{v}}))$ fulfilling (8), we prove that $\|\mathbf{u}^{(k+1)}-\mathbf{u}^{(k)}\|_\infty<\|\mathbf{u}^{(k)}-\mathbf{u}^{(k-1)}\|_\infty$ if ρ further satisfies (9).

Similar to the proof of self-mapping, we have

$$\begin{aligned}
&\mathbf{u}^{(k+1)}-\mathbf{u}^{(k)}\\
&=\mathbf{W}^{-1}\mathbf{Y}_{LL}^{-1}\overline{\mathbf{W}}^{-1}\left(\mathsf{diag}(\overline{\mathbf{u}}^{(k)})^{-1}\overline{\mathbf{s}^{\mathbf{Y}}}-\mathsf{diag}(\overline{\mathbf{u}}^{(k-1)})^{-1}\overline{\mathbf{s}^{\mathbf{Y}}}\right)\\
&+\mathbf{W}^{-1}\mathbf{Y}_{LL}^{-1}\mathbf{H}^{T}\left(\mathsf{diag}(\mathbf{H}\overline{\mathbf{W}}\overline{\mathbf{u}}^{(k)})^{-1}\overline{\mathbf{s}^{\Delta}}-\mathsf{diag}(\mathbf{H}\overline{\mathbf{W}}\overline{\mathbf{u}}^{(k-1)})^{-1}\overline{\mathbf{s}^{\Delta}}\right).
\end{aligned}$$

Then, via derivations analogues to (22) and (24), there is

$$\begin{aligned}
&\|\mathbf{u}^{(k+1)}-\mathbf{u}^{(k)}\|_\infty\\
&\le\xi^{Y}(\mathbf{s})\max_{j\in\{1,\dots,3N\}}|(\mathbf{u}^{(k)})_j-(\mathbf{u}^{(k-1)})_j|/[|(\mathbf{u}^{(k)})_j||(\mathbf{u}^{(k-1)})_j|]\\
&+\xi^{\Delta}(\mathbf{s})\max_{j\in\{1,\dots,3N\}}\frac{|(\mathbf{H}\mathbf{W}\mathbf{u}^{(k)})_j-(\mathbf{H}\mathbf{W}\mathbf{u}^{(k-1)})_j|/(\mathbf{L}|\mathbf{w}|)_j}{\frac{|(\mathbf{H}\mathbf{W}\mathbf{u}^{(k)})_j|}{(\mathbf{L}|\mathbf{w}|)_j}\frac{|(\mathbf{H}\mathbf{W}\mathbf{u}^{(k-1)})_j|}{(\mathbf{L}|\mathbf{w}|)_j}}\\
&\le\left(\frac{\xi^{Y}(\mathbf{s})}{(\alpha(\widehat{\mathbf{v}})-\rho)^2}+\frac{\xi^{\Delta}(\mathbf{s})}{(\beta(\widehat{\mathbf{v}})-\rho)^2}\right)\|\mathbf{u}^{(k)}-\mathbf{u}^{(k-1)}\|_\infty. \quad (28)
\end{aligned}$$

Clearly, $\|\mathbf{u}^{(k+1)}-\mathbf{u}^{(k)}\|_\infty<\|\mathbf{u}^{(k)}-\mathbf{u}^{(k-1)}\|_\infty$ if ρ further satisfies (9).

C. Proof of Theorem 2

We show that conditions (11) and (12) imply conditions (8) and (9) of Theorem 1. From the proof of Lemma 1 in [8], whenever (11) and (12) are satisfied, we have

$$\rho^2-\rho((\gamma(\widehat{\mathbf{v}}))^2-\xi(\widehat{\mathbf{s}}))/\gamma(\widehat{\mathbf{v}})+\xi(\mathbf{s}-\widehat{\mathbf{s}})\le0 \quad (29)$$

for $\rho\in[\rho^{\dagger}(\widehat{\mathbf{v}},\widehat{\mathbf{s}},\mathbf{s}),\rho^{\ddagger}(\widehat{\mathbf{v}},\widehat{\mathbf{s}})]\subseteq(0,\gamma(\widehat{\mathbf{v}}))$. After re-organization, the above inequality becomes

$$\frac{\xi(\mathbf{s}-\widehat{\mathbf{s}})+\rho\xi(\widehat{\mathbf{s}})/\gamma(\widehat{\mathbf{v}})}{\gamma(\widehat{\mathbf{v}})-\rho}\le\rho. \quad (30)$$

Note that

$$\frac{\xi^{Y}(\mathbf{s}-\widehat{\mathbf{s}})+\frac{\xi^{Y}(\widehat{\mathbf{s}})}{\alpha(\widehat{\mathbf{v}})}\rho}{\alpha(\widehat{\mathbf{v}})-\rho}+\frac{\xi^{\Delta}(\mathbf{s}-\widehat{\mathbf{s}})+\frac{\xi^{\Delta}(\widehat{\mathbf{s}})}{\beta(\widehat{\mathbf{v}})}\rho}{\beta(\widehat{\mathbf{v}})-\rho}\le\frac{\xi(\mathbf{s}-\widehat{\mathbf{s}})+\frac{\xi(\widehat{\mathbf{s}})}{\gamma(\widehat{\mathbf{v}})}\rho}{\gamma(\widehat{\mathbf{v}})-\rho}, \quad (31)$$

and hence (8) is satisfied. Namely, $\widetilde{\mathbf{G}}_{\mathbf{s}^{Y}\mathbf{s}^{\Delta}}(\mathbf{u})$ is a self-mapping on domain $\widetilde{\mathcal{D}}_\rho(\widehat{\mathbf{u}})$ for $\rho\in[\rho^{\dagger}(\widehat{\mathbf{v}},\widehat{\mathbf{s}},\mathbf{s}),\rho^{\ddagger}(\widehat{\mathbf{v}},\widehat{\mathbf{s}})]$.

Further, taking into account (12) and the fact that $\xi(\cdot)$ is a norm (cf. Lemma 1), we have

$$\begin{aligned}
\xi(\mathbf{s})&\le\xi(\mathbf{s}-\widehat{\mathbf{s}})+\xi(\widehat{\mathbf{s}})<\frac{1}{4}\left(\frac{(\gamma(\widehat{\mathbf{v}}))^2-\xi(\widehat{\mathbf{s}})}{\gamma(\widehat{\mathbf{v}})}\right)^2+\xi(\widehat{\mathbf{s}})\\
&=\frac{1}{4}\left(\frac{(\gamma(\widehat{\mathbf{v}}))^2+\xi(\widehat{\mathbf{s}})}{\gamma(\widehat{\mathbf{v}})}\right)^2=(\gamma(\widehat{\mathbf{v}})-\rho^{\ddagger}(\widehat{\mathbf{v}},\widehat{\mathbf{s}}))^2. \quad (32)
\end{aligned}$$

Then, it is easy to see that

$$\frac{\xi^{Y}(\mathbf{s})}{(\alpha(\widehat{\mathbf{v}})-\rho)^2}+\frac{\xi^{\Delta}(\mathbf{s})}{(\beta(\widehat{\mathbf{v}})-\rho)^2}\le\frac{\xi(\mathbf{s})}{(\gamma(\widehat{\mathbf{v}})-\rho)^2}<\frac{\left(\gamma(\widehat{\mathbf{v}})-\rho^{\ddagger}(\widehat{\mathbf{v}},\widehat{\mathbf{s}})\right)^2}{(\gamma(\widehat{\mathbf{v}})-\rho)^2}\le1$$

for $\rho\in[\rho^{\dagger}(\widehat{\mathbf{v}},\widehat{\mathbf{s}},\mathbf{s}),\rho^{\ddagger}(\widehat{\mathbf{v}},\widehat{\mathbf{s}})]$. It implies that $\widetilde{\mathbf{G}}_{\mathbf{s}^{Y}\mathbf{s}^{\Delta}}(\mathbf{u})$ is also a contraction mapping on $\widetilde{\mathcal{D}}_\rho(\widehat{\mathbf{u}})$ with $\rho\in[\rho^{\dagger}(\widehat{\mathbf{v}},\widehat{\mathbf{s}},\mathbf{s}),\rho^{\ddagger}(\widehat{\mathbf{v}},\widehat{\mathbf{s}})]$. This completes the proof.

D. Proof of Theorem 3

The proof is an extension of the proof of Theorem 1 in [16]. Because the system is linear with respect to the rectangular coordinates and there are as many unknowns as equations, the result is equivalent to showing that the corresponding homogeneous system of equations has only the trivial solution

(see, e.g., [22]). Note that the homogeneous system is the same for every column of (15) and is given by

$$\begin{aligned}&\mathsf{diag}\left(\mathbf{H}^{\mathsf{T}}\overline{\mathbf{i}^{\Delta}}\right)\boldsymbol{\Delta}_V + \mathsf{diag}(\mathbf{v})\mathbf{H}^{\mathsf{T}}\overline{\boldsymbol{\Delta}}_I,\\ &\quad = \mathsf{diag}(\mathbf{v})\overline{\mathbf{Y}}_{LL}\overline{\boldsymbol{\Delta}}_V + \mathsf{diag}(\overline{\mathbf{Y}}_{L0}\overline{\mathbf{v}}_0 + \overline{\mathbf{Y}}_{LL}\overline{\mathbf{v}})\boldsymbol{\Delta}_V \quad (33a)\\ &\mathbf{0} = \mathsf{diag}\left(\mathbf{H}\mathbf{v}\right)\overline{\boldsymbol{\Delta}}_I + \mathsf{diag}(\overline{\mathbf{i}^{\Delta}})\mathbf{H}\boldsymbol{\Delta}_V, \quad (33b)\end{aligned}$$

where $\boldsymbol{\Delta}_V, \boldsymbol{\Delta}_I$ are solution vectors.

For brevity, we first focus on condition (ii) of the theorem. Assume, by the way of contradiction, that there exists a solution $\boldsymbol{\Delta}' := ({\boldsymbol{\Delta}'}_V^{\mathsf{T}}, {\boldsymbol{\Delta}'}_I^{\mathsf{T}})^{\mathsf{T}}$ to (33) such that $\boldsymbol{\Delta}' \neq 0$. In particular, any vector $\boldsymbol{\Delta}^{\epsilon} := \epsilon\boldsymbol{\Delta}'$ for $\epsilon > 0$ is a solution to (33).

Now consider two power networks with the same topology but different voltages and between-phase currents. In particular, let $\mathbf{v}_1^{\epsilon} = \mathbf{v} + \boldsymbol{\Delta}_V^{\epsilon}$, $\mathbf{i}_1^{\epsilon,\Delta} = \mathbf{i}^{\Delta} + \boldsymbol{\Delta}_I^{\epsilon}$, $\mathbf{v}_2^{\epsilon} = \mathbf{v} - \boldsymbol{\Delta}_V^{\epsilon}$, and $\mathbf{i}_2^{\epsilon,\Delta} = \mathbf{i}^{\Delta} - \boldsymbol{\Delta}_I^{\epsilon}$, while $\mathbf{v}_0$ is the same in both networks. Note that there exists $\epsilon_1 > 0$ such that for all $\epsilon < \epsilon_1$, $\mathbf{v}_1^{\epsilon}, \mathbf{v}_2^{\epsilon} \in \mathcal{D}_{\rho^{\dagger}}(\mathbf{v})$, where $\mathcal{D}_{\rho^{\dagger}}$ is defined in (10) (with $\widehat{\mathbf{v}} = \mathbf{v}$).

Let $\mathbf{s}_1^{\epsilon,Y}, \mathbf{s}_1^{\epsilon,\Delta}, \mathbf{s}_2^{\epsilon,Y}, \mathbf{s}_2^{\epsilon,\Delta}$ be the corresponding power injections. Using (1), we obtain that

$$\begin{aligned}\mathbf{s}_1^{\epsilon,Y} - \mathbf{s}_2^{\epsilon,Y} &= 2\Big(\mathsf{diag}(\mathbf{v})\overline{\mathbf{Y}}_{LL}\overline{\boldsymbol{\Delta}}_V^{\epsilon}\\ &\quad + \mathsf{diag}(\overline{\mathbf{Y}}_{L0}\overline{\mathbf{v}}_0 + \overline{\mathbf{Y}}_{LL}\overline{\mathbf{v}})\boldsymbol{\Delta}_V^{\epsilon} - \mathsf{diag}\left(\mathbf{H}^{\mathsf{T}}\overline{\mathbf{i}^{\Delta}}\right)\boldsymbol{\Delta}_V^{\epsilon}\\ &\quad - \mathsf{diag}(\mathbf{v})\mathbf{H}^{\mathsf{T}}\overline{\boldsymbol{\Delta}}_I^{\epsilon}\Big),\\ \mathbf{s}_1^{\epsilon,\Delta} - \mathbf{s}_2^{\epsilon,\Delta} &= 2\left(\mathsf{diag}\left(\mathbf{H}\mathbf{v}\right)\overline{\boldsymbol{\Delta}}_I^{\epsilon} + \mathsf{diag}(\overline{\mathbf{i}^{\Delta}})\mathbf{H}\boldsymbol{\Delta}_V^{\epsilon}\right),\end{aligned}$$

which by (33) implies that $\mathbf{s}_1^{\epsilon,Y} = \mathbf{s}_2^{\epsilon,Y}$ and $\mathbf{s}_1^{\epsilon,\Delta} = \mathbf{s}_2^{\epsilon,\Delta}$.

Let $\mathbf{s}^{\epsilon} := ((\mathbf{s}_1^{\epsilon,Y})^{\mathsf{T}}, (\mathbf{s}_1^{\epsilon,\Delta})^{\mathsf{T}})^{\mathsf{T}}$. It is easy to see that there exists $\epsilon_2 > 0$ such that for all $\epsilon < \epsilon_2$, $\mathbf{s}^{\epsilon}$ satisfies (12) (with $\widehat{\mathbf{s}} = \mathbf{s}$). Let $\epsilon^* = \min\{\epsilon_1, \epsilon_2\}$. Then, by Theorem 2, we have that for any $\epsilon \in (0, \epsilon^*)$, $\mathbf{v}_1^{\epsilon} = \mathbf{v}_2^{\epsilon}$ and $\mathbf{i}_1^{\epsilon,\Delta} = \mathbf{i}_2^{\epsilon,\Delta}$. This is equivalent to having $\boldsymbol{\Delta}_V^{\epsilon} = \mathbf{0}$ and $\boldsymbol{\Delta}_I^{\epsilon} = \mathbf{0}$, which is a contradiction to our assumption that $\boldsymbol{\Delta}^{\epsilon} \neq 0$. This completes the proof.

Note that the above result follows exactly in the same way under the nonsingularity of the Jacobian at the operating point (namely, condition (i) of the theorem). Indeed, if $\mathbf{J}$ is invertible, we can apply the inverse function theorem. As a consequence, the system of the power-flow equations is locally invertible in a neighbourhood around the current operating point. Now, we take ϵ arbitrarily small, such that $\mathbf{y}_{\ell}^{\epsilon} := \left(\Re\{\mathbf{v}_{\ell}^{\epsilon}\}^{\mathsf{T}}, \Im\{\mathbf{v}_{\ell}^{\epsilon}\}^{\mathsf{T}}, \Re\{\mathbf{i}_{\ell}^{\epsilon,\Delta}\}^{\mathsf{T}}, \Im\{\mathbf{i}_{\ell}^{\epsilon,\Delta}\}^{\mathsf{T}}\right)^{\mathsf{T}}$, $\ell = 1, 2$, belong to this neighbourhood. As the powers that correspond to $\mathbf{y}_1^{\epsilon}$ and $\mathbf{y}_2^{\epsilon}$ are exactly the same, then it follows that the voltage profile of these networks must be exactly the same, and the result follows.

E. Proof of Theorem 4

Note that (17) is in fact a single iteration of the fixed-point equation initialized at $\widehat{\mathbf{v}}$. Therefore, by identifying $\mathbf{v}^{(0)} = \widehat{\mathbf{v}}$ and $\mathbf{v}^{(1)} = \widetilde{\mathbf{v}}$, we have that

$$\|\widetilde{\mathbf{v}} - \mathbf{v}\|_{\infty} \leq q\|\widehat{\mathbf{v}} - \mathbf{v}\|_{\infty} \leq q\|\mathbf{w}\|_{\infty}\|\widehat{\mathbf{u}} - \mathbf{u}\|_{\infty} \leq q\|\mathbf{w}\|_{\infty}\rho^{\dagger},$$

where $q < 1$ is the contraction coefficient given in the proof of Theorem 2 – cf. (28); the first inequality follows by the Banach fixed point theorem; the second inequality holds by definition of $\mathbf{v} = \mathbf{W}\mathbf{u}$; and the last inequality follows because $\mathbf{v} \in \mathcal{D}_{\rho^{\dagger}}(\widehat{\mathbf{v}})$ (cf. (10)).

REFERENCES

[1] W. H. Kersting, *Distribution System Modeling and Analysis*. 2nd ed., Boca Raton, FL: CRC Press, 2007.

[2] Y. Wang and W. Xu, "The existence of multiple power flow solutions in unbalanced three-phase circuits," *IEEE Transactions on Power Systems*, vol. 18, no. 2, pp. 605–610, May 2003.

[3] B. K. Johnson, "Extraneous and false load flow solutions," *IEEE Transactions on Power Apparatus and Systems*, vol. 96, no. 2, pp. 524–534, 1977.

[4] H. D. Nguyen and K. S. Turitsyn, "Appearance of multiple stable load flow solutions under power flow reversal conditions," in *2014 IEEE PES General Meeting — Conference Exposition*, 2014, pp. 1–5.

[5] J. W. Simpson-Porco, "A theory of solvability for lossless power flow equations - part I: Fixed-point power flow," *IEEE Transactions on Power Systems*, 2016, [Online] Available at: https://arxiv.org/pdf/1701.02045.pdf.

[6] S. Bolognani and S. Zampieri, "On the existence and linear approximation of the power flow solution in power distribution networks," *IEEE Trans. on Power Systems*, 2015.

[7] S. Yu, H. D. Nguyen, and K. S. Turitsyn, "Simple certificate of solvability of power flow equations for distribution systems," in *2015 IEEE Power Energy Society General Meeting*, 2015, pp. 1–5.

[8] C. Wang, A. Bernstein, J.-Y. Le Boudec, and M. Paolone, "Explicit Conditions on Existence and Uniqueness of Load-Flow Solutions in Distribution Networks," *IEEE Transactions on Smart Grid*, 2016.

[9] C. Wang, A. Bernstein, J.-Y. Le Boudec, and M. Paolone, "Existence and uniqueness of load-flow solutions in three-phase distribution networks," *IEEE Transactions on Power Systems*, vol. PP, no. 99, pp. 1–1, 2016.

[10] M. Bazrafshan and N. Gatsis, "Convergence of the Z-bus method for three-phase distribution load-flow with ZIP loads," 2016, [Online] Available at: https://arxiv.org/abs/1605.08511.

[11] T. H. Chen, M. S. Chen, K. J. Hwang, P. Kotas, and E. A. Chebli, "Distribution system power flow analysis-a rigid approach," *IEEE Transactions on Power Delivery*, vol. 6, no. 3, pp. 1146–1152, Jul 1991.

[12] D. Borzacchiello, F. Chinesta, M. Malik, R. Garca-Blanco, and P. Diez, "Unified formulation of a family of iterative solvers for power systems analysis," *Electric Power Systems Research*, vol. 140, pp. 201 – 208, 2016.

[13] R. C. Dugan and T. E. McDermott, "An open source platform for collaborating on smart grid research," in *2011 IEEE Power and Energy Society General Meeting*, July 2011, pp. 1–7.

[14] S. H. Low, "Convex relaxation of optimal power flow – part I: Formulations and equivalence," *IEEE Transactions on Control of Network Systems*, vol. 1, no. 1, pp. 15–27, March 2014.

[15] S. Guggilam, E. Dall'Anese, Y. Chen, S. Dhople, and G. B. Giannakis, "Scalable optimization methods for distribution networks with high PV integration," *IEEE Transactions on Smart Grid*, 2015, submitted.

[16] K. Christakou, J.-Y. Le Boudec, M. Paolone, and D.-C. Tomozei, "Efficient Computation of Sensitivity Coefficients of Node Voltages and Line Currents in Unbalanced Radial Electrical Distribution Networks," *IEEE Transactions on Smart Grid*, vol. 4, no. 2, pp. 741–750, 2013.

[17] S. Dhople, S. Guggilam, and Y. Chen, "Linear approximations to ac power flow in rectangular coordinates," *Allerton Conference on Communication, Control, and Computing , in Press*, 2015.

[18] S. Bolognani and F. Dörfler, "Fast power system analysis via implicit linearization of the power flow manifold," *Allerton Conference on Communication, Control, and Computing , in Press*, 2015.

[19] A. Bernstein, L. E. Reyes Chamorro, J.-Y. Le Boudec, and M. Paolone, "A composable method for real-time control of active distribution networks with explicit power set points. part I: Framework," *Electric Power Systems Research*, vol. 125, no. August, pp. 254–264, 2015.

[20] E. Dall'Anese and A. Simonetto, "Optimal power flow pursuit," *IEEE Transactions on Smart Grid*, 2016, to appear.

[21] W. H. Kersting, "Radial distribution test feeders," in *IEEE Power Engineering Society Winter Meeting*, vol. 2, 2001, pp. 908–912.

[22] R. A. Horn and C. R. Johnson, *Matrix analysis*. Cambridge University Press, 1990.